ISSN (ONLINE) : 2395-695X
ISSN (PRINT) : 2395-695X
Available online at www.ijarbest.com
International Journal of Advanced Research in Biology, Ecology, Science and Technology (IJARBEST)
Vol. 1, Issue 8, November 2015

Pixel Based A'trous Wavelet Transform for Satellite Image Fusion

Jeyaseeli Rashmi I , Jothi Shalini K G
PG scholar, Applied Electronics, V V College of Engineering, Tisaiyanlvilai.
PG scholar, Communication Systems, Francis Xavier Engineering College, Tirunelveli.
jrashmarose@gmail.com
jothishalini25@gmail.com

Abstract—The task of enhancing the perception of a scene by combining information captured from different image sensors is usually known as multisensor image fusion. This paper presents an area-based image fusion algorithm to merge SAR (Synthetic Aperture Radar) and optical images. Segmentation into active and inactive areas is then performed on the SAR texture image for selective injection of the SAR image into the panchromatic (PAN) image. An integrated image based on these two images is generated by the novel area-based fusion scheme, which imposes different fusion rules for each segmented area. Experimental results demonstrate that the proposed method shows better performance than other fusion algorithms and has the potential to be applied to the multisensor fusion of SAR and optical images.

Index Terms – Area-based fusion scheme, multisensor image fusion, wavelet transform.

I. INTRODUCTION

With the recent, rapid developments in the field of sensing technologies, multisensor imaging systems are being used in a growing number of fields, such as in remote sensing and military applications. Multisensor image fusion, which is defined as the process of combining relevant information from two or more images into a single image, has been receiving increasing attention in the remote sensing research community due to the increasing availability of space borne imaging sensors [1],[2]. The objective of multisensor image fusion is to combine complementary information from multi- sensor images of the same scene into a single image to obtain data that is more useful than the data from any of the individual source images by reducing imprecision and uncertainty in the spatial properties and maintaining completeness of the spectral information [2]. Such fused images should be more useful for further image processing tasks such as image segmentation, object identification, and regional change detection [3]–[6]. This type of image fusion is also called pixel level multisensor image fusion [2].Various multisensor image fusion schemes have been developed over the past few years. A comparative evaluation of ten fusion techniques for testing the effectiveness of fusion TerraSAR-X and SPOT 5 images are described in [7]. It is shown that the Ehlers fusion method, which is based on an intensity-hue-saturation (IHS) transform coupled with Fourier domain filtering, is more efficient for multisensor image fusion than other fusion methods. A multisensor image fusion algorithm based on intensity modulation was proposed by Alparone et al. [8] for integrating PAN and SAR features into MS images; it relies on SAR texture extracted by rationing the despeckled SAR image to its low-pass approximation with "atrous" wavelet de- composition. It can adjust the amount of integration using a threshold to avoid full integration of SAR features. Chibani [9] integrated PAN and SAR features into MS images using the modified Brovey transform (MBT) and "atrous" wavelet decomposition conjointly. The MBT is based on the local modulation of each MS image by the ratio of the new intensity and the initial intensity components. The new intensity component was produced by combining PAN and SAR features through a feature selection rule. Hong et al. [10] proposed a fusion method, which is based on the integration of wavelet transform and IHS transform, to fuse high spatial resolution SAR images with moderate spatial resolution MS images. In the fusion process proposed by Hong et al. [10], a new

ISSN (ONLINE) : 2395-695X
ISSN (PRINT) : 2395-695X
Available online at www.ijarbest.com
International Journal of Advanced Research in Biology, Ecology, Science and Technology (IJARBEST)
Vol. 1, Issue 8, November 2015

wavelet-based approximation image, obtained using a weighted combination of SAR features and the intensity component of MS images, is used to avoid over-injection of the SAR intensity information. A block regression-based fusion method of optical and SAR imagery was proposed by Zhang et al. [11], which is a technique based on multiple linear regression of block regions to combine these two types of images for feature enhancement. The ensemble empirical mode decomposition (EMD) has recently been employed for multisensor image fusion, in which the spatial details from SAR images were extracted using "atrous" wavelet transform, and the EMD was used to fuse the approximation plane of the SAR image with the MS image, instead of performing a whole substitution [12]. To address this issue, we first segmented the image into two areas using the SAR texture information: i) an active area represented by the homogenous parts of the image and ii) an inactive area represented by the heterogeneous parts of the image. These areas were then fused using different fusion rules to improve fusion quality. The general frame work is briefly described and our hybrid procedures are defined in Section II. In Section III, we compare the fusion quality obtained using our method with existing fusion methods. Conclusions are presented in Section IV.

II. FUSION PROCEDURE

The basic structure of the proposed fusion scheme consists of four steps. The process of extracting the inactive area from the SAR image, which is based on texture segmentation with a quadtree data structure, is then developed to create a binary decision map (mask image) that is used to apply a different fusion rule within the detected inactive areas in a subsequent image fusion process. Finally is the process of integrating PAN and SAR images in which the features of these two images are combined into a fused image (PS) through a novel feature selection rule. In this section, we propose an algorithm that can extract inactive areas from the VHR (Very High Resolution) SAR image. The texture image is first produced using the gray level co-occurrence matrix (GLCM), which was first introduced by Haralick [22], and this image is then partitioned into a set of block regions with various sizes through the process of texture segmentation, based on the quadtree data structure. Finally, all pixels included within the smallest region in the segmented regions are extracted as inactive areas.

A co-occurrence matrix describes how often one gray level appears in a specified spatial relationship with another gray level. The entry (i,j)at of the GLCM indicates the number of occurrences of the pair of gray levels and that are a distance apart along a given direction. After construction of the GLCM, we choose the entropy measure of GLCM texture descriptor, which is widely used to describe image texture. Entropy measures the randomness of the elements of the co-occurrence matrix; it is maximum when elements in the matrix are equal, while is equal to 0 if all elements are different.

Entropy acts similar to correlation matrix. By using the entropy, similar and dissimilar pixels can be classified in an effective manner. The entropy equation is as follow:

$$Ent = -\sum_{i}^{K}\sum_{j}^{K} P_{ij} \log_2(P_{ij})$$

Where P_{ij} represents the elements of the co-occurrence matrix, and K is the number of gray levels used to reduce the size of the matrix. Once the texture feature is generated from GLCM, Quadtree structured split and merge (QSM), which is a popular approach for image segmentation because of its simplicity and computational efficiency [23], is carried out to extract inactive areas in the texture map. The QSM is constructed by recursively decomposing the image into four equal sized regions in a top down fashion until the minimum accepted region size is achieved. The top-down approach begins with the whole image representing a single region and successively divides the image into four sub-regions based on the degree of homogeneity of the sub-regions' feature values. Once splitting has been accomplished, a merging process is then performed. Pairs of adjacent regions are compared and merged if their union satisfies the homogeneity criterion.

ISSN (ONLINE) : 2395-695X
ISSN (PRINT) : 2395-695X
Available online at www.ijarbest.com
International Journal of Advanced Research in Biology, Ecology, Science and Technology (IJARBEST)
Vol. 1, Issue 8, November 2015

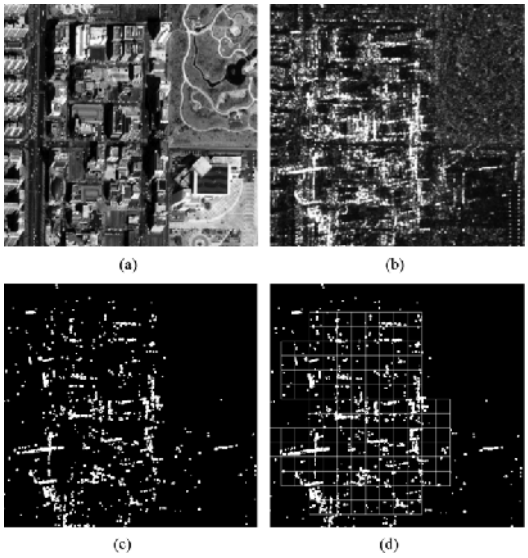

Fig. 1. Inactive area extraction results: (a) IKONOS PAN image, (b) TerraSAR-X image, (c) texture image extracted from TerraSAR-X, and (d) the extraction results of the inactive area.

Fig. 1 shows an example of the extraction of the inactive area from a SAR image (Fig. 1(b)). Fig. 1(c) illustrates the texture map obtained by applying GLCM to the SAR image. In Fig. 1(d), a patch of extraction results for the inactive area extracted from the texture map is shown, and the boundaries of the extracted regions were superimposed on the texture map for visual inspection. The extracted regions correspond approximately to the coverage of the densely populated urban area in the PAN image (Fig. 1(a))). It is worth noting that the area corresponding to a large building with a flat roof in the lower left corner of Fig. 1(a) was not extracted as an inactive area. This is because this type of building has homogenous characteristics due to the single bounce backscattering effect in the SAR image, as shown Fig. 1(b). The fusion of this area does not substantially affect the fusion quality of the SAR and the optical image because the intensity variations between two images in this area are relatively small and consistent.

A. The"a trous" Wavelet Transformation

The wavelet transform is a very effective tool for time frequency or phase-space analysis of signals with multiple scales of resolution. Among the wavelet transform's numerous applications, multiresolution decomposition of an image provides a suitable tool for pixel-level image fusion studies since it can preserve the original image's fine details and spectral information. The wavelet transform can be derived through several different techniques, but each of these techniques is best suited for a particular type of problem [24]. Generally, the widely used Mallet [25] algorithm is not shift-invariant because of an underlying down-sampling process in discrete wavelet transform (DWT) that creates artifacts due to aliasing in the fused image.

This is particularly undesirable when the source images, like multisensor images, cannot be perfectly registered [26]. In this paper, we thus used "a'trous" wavelet transform (AWT) [27], which can obtain a shift-invariant discrete wavelet decomposition for images. The AWT is very similar to the Laplacian Pyramid (LP) except that the low pass images are never subsampled. Thus, the approximation and detail images at consecutive scales are the same size as the original image. A'trous wavelet transform is a extremely powerful processing tool that performs a wide variety of noise reduction and detail enhancement tasks. Generally, the widely used Mallet algorithm is not shift-invariant that creates artifacts due to aliasing in the fused image. This is particularly undesirable .The AWT is very similar to the Laplacian Pyramid (LP) except that the low pass images are never sub sampled.

The a'trous (with hole) algorithm of DWT is an elegant and powerful tool for multi scale (multi resolution) analysis of image. . With this method , we can perform hierarchical decomposition of an image into series of scale layers, also known as wavelet planes. Each layer contains only structures within a given range of characteristic dimensional scales in the space of a scaling function. In this method noise can be removed without affecting the structures. Detail enhancement can be carried out with high accuracy. A'trous wavelet is a non decimated wavelet transform.

ISSN (ONLINE) : 2395-695X
ISSN (PRINT) : 2395-695X
Available online at www.ijarbest.com
International Journal of Advanced Research in Biology, Ecology, Science and Technology (IJARBEST)
Vol. 1, Issue 8, November 2015

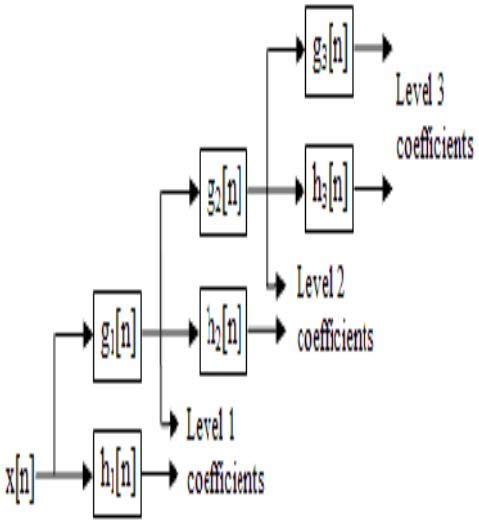

Fig 2. A'trous wavelet transform

B. Integration Scheme of PAN and SAR Images

The basic idea underlying our proposed fusion method is to perform selective fusion in the inactive areas instead of fully integrating SAR features into PAN images because the SAR features of inactive areas have a negative effect on the interpretability of these areas in the fused image. The AWT is first performed to create wavelet decomposition on each source image. Each wavelet approximation image is then combined by the feature selection rule that takes into account the non-active area in the process of merging the two images into one. Finally, an integrated map, combining PAN and SAR information, is generated by performing the inverse AWT. The whole procedure can be summarized as follows:

1) Apply histogram matching, defined in (10), to match the histogram of the SAR to that of the PAN image; this adjusts the backscatter intensities of the SAR image based on the grayscale values of the PAN image.

2) Decompose both the SAR and PAN into wavelet planes using AWT two-level decomposition is applied.

3)A new approximation image is generated through a feature selection rule to integrate PAN and SAR features and then substitutes the approximation image of the PAN. The feature selection rule is defined by (11) and (12). (In this step, the approximation image of the SAR is partially combined with that of the PAN, whereas the detail images of the PAN wavelet decomposition remain unchanged).

4)The stripe boundary error, caused by feature value changes at the boundary of the inactive area, exists in the new approximation image. This error can be substantially reduced by applying the mean filter (5 5 window) along the boundary.

5) An inverse AWT is performed to obtain a fused image that has a similar gray value distribution to that of the SAR image in the active area and that contains the same spatial details of the original PAN image in the whole image.

Histogram matching can be used to normalize two images that were acquired at the same location but by different sensors or under different atmospheric conditions or global illumination [28]. Histogram matching is performed on the SAR image to match its mean and standard deviation to those of the PAN image.

$$S_H = \frac{\sigma_{PAN}}{\sigma_{SAR}} X\,(SAR(p) - \mu_{SAR}) + \mu_{PAN}$$

where S_H is the histogram-matched SAR image. SAR(P) is the SAR image; μSAR and μPAN are the means of the SAR and PAN images, respectively; σSAR and σPAN are the standard deviations of the SAR and PAN images, respectively. The method to generate the new approximation image can be expressed as:

$$a_N(PS) = \begin{cases} a_N(P) & , \quad if\ M(p) = true \\ a_N(P)\ X\ w_1 + a_N(S) X\ w_2 & , \quad Otherwise. \end{cases}$$

Where $a_N(P)$ and $a_N(S)$ are the approximation images of PAN and SAR images, respectively.

III. EXPERIMENTAL RESULTS

In this paper, we used satellite images from IKONOS, KOMPSAT-2,CartoSat-2A,ERS and TerraSAR-X to verify the quality of fused image generated by our algorithm. The study site for evaluating the proposed method is located in Malaysia, Washington Dc,Singapore,Mumbai. They are urban regions that are mostly comprised of buildings, roads, vegetation, and low mountains.

A.Results for different datasets

Dataset 1 (IKONOS)

Dataset1 consists of SAR and Panchromatic image acquired during April,1999. The fused image of SAR and panchromatic image is shown in Fig. 3. This is the IKONOS satellite image. IKONOS satellite uses Synthetic Aperture Radar for image acquisition. While performing the fusion with

ISSN (ONLINE) : 2395-695X
ISSN (PRINT) : 2395-695X
Available online at www.ijarbest.com
International Journal of Advanced Research in Biology, Ecology, Science and Technology (IJARBEST)
Vol. 1, Issue 8, November 2015

panchromatic image, resolution increases and error decreases. This is mainly used for remote sensing applications.

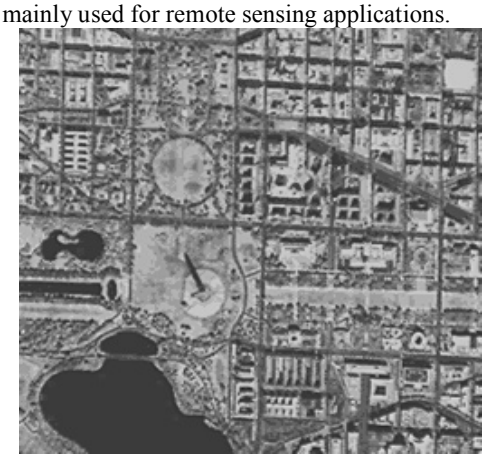

Fig 3.Final fused image of IKONOS

Dataset -2 (KOMPSAT)

Dataset2 consists of SAR and Panchromatic image acquired during 2000.The fused image is shown in Fig. 4

Fig 4.final fused image of Washington (KOMPSAT)

Dataset-3(CartoSat 2A)

Dataset3 consists of SAR and Panchromatic image acquired during April,2008 .Fig 4.11 is the SAR image .Fig 4.12 is the Panchromatic image.Fig:4.11 final fused image of Mumbai(CartoSat 2A-ISRO)

Fig 5.fused image of CartoSat 2A

Dataset-4

Dataset5 consists of SAR and Panchromatic image acquired during Sep,1993. Here Washington Dc image is given. This is the most frequentl used image for satellite image processing research purpose.

Fig 6.Final fused image of Washington Dc

B.Performance measures

In the proposed PAN -SAR fusion algorithm, we can arbitrarily choose the fusion factor and the block size (selection rule) based on our requirement and condition of the input images. Quality and error components of the image varies based on the fusion factor and the block size used .The performance of the Fusion algorithm is tested using different data sets and the readings are tabulated and plotted.

For dataset1, the performance measures like BIAS, CC, Mean Quality, RASE , RMSE are computed for different values of the fusion factor for a block size of 4x4 and tabulated in Table 1.

ISSN (ONLINE) : 2395-695X
ISSN (PRINT) : 2395-695X
Available online at www.ijarbest.com
International Journal of Advanced Research in Biology, Ecology, Science and Technology (IJARBEST)
Vol. 1, Issue 8, November 2015

C.Comparison Plots

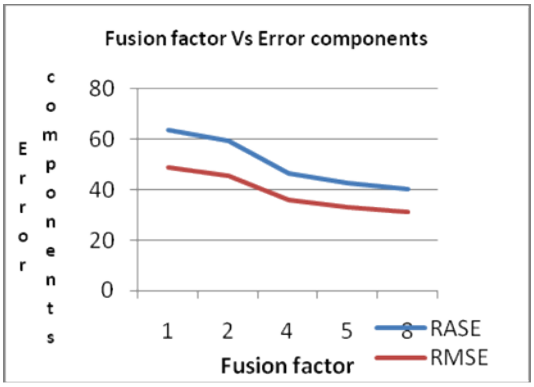

Fig 7..Fusion factor vs Error components of KOMPSAT washington

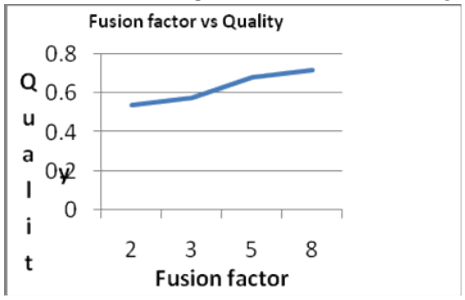

Fig 8.Fusion factor vs Quality of fused image of CartoSat 2A mumbai

In figure 7 and eight comparison plots are given. Here, based on fusion factor quality of the images and error factor in the images are compared. When the fusion factor increases, quality of the image also increases. At the same time error components are decreased

D.Comparison with standard method

TABLE I
PERFORMANCE MEASURES OF DATASET 1

FUSION FACTOR	1	2	4	5	8
BIAS	-0.34	-0.34	-0.23	-0.20	-0.23
CC	0.56	0.65	0.78	0.83	0.89
MEAN QUALITY	0.48	0.57	0.68	0.733	0.80
RASE	63.53	59.5	46.62	42.87	40.30
RMSE	48.87	45.77	35.86	32.97	31.01

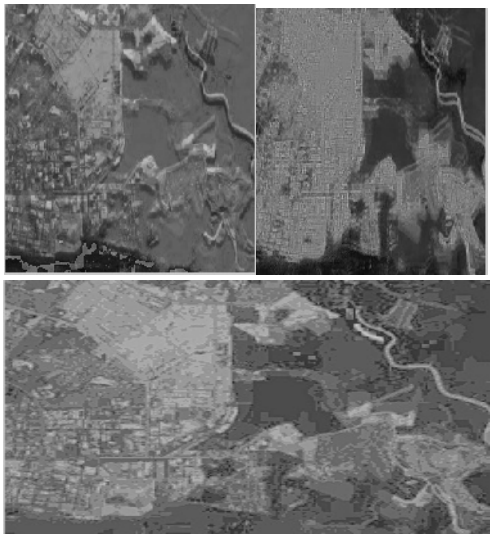

Fig 9. KOMPSAT-Singapore a)IHS b)DWT c)A'trous

E.Other Comparisons

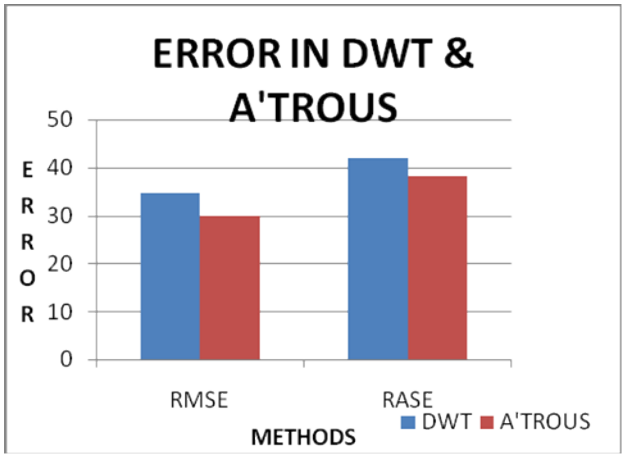

Fig 10.Errors in DWT & A'TROUS

ISSN (ONLINE) : 2395-695X
ISSN (PRINT) : 2395-695X
Available online at www.ijarbest.com
International Journal of Advanced Research in Biology, Ecology, Science and Technology (IJARBEST)
Vol. 1, Issue 8, November 2015

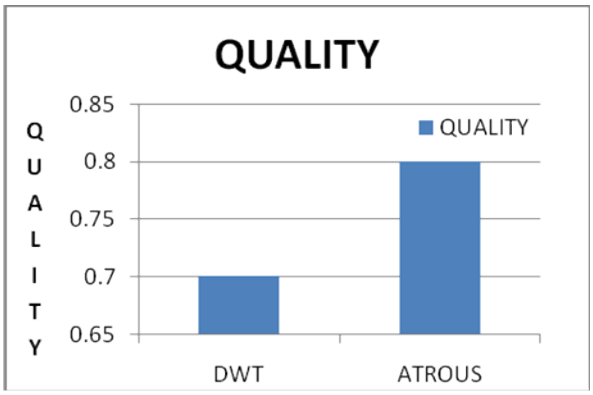

Fig 11.Quality in DWT & A'TROUS

IV. CONCLUSION

In this paper, a new method is proposed for multisensor image fusion where an area-based fusion rule was used to address the fusion of optical and SAR images. In conclusion, by incorporatingonly the SAR features of active (homogeneous) areas into optical images, we are able to efficiently increase the interpretability of the fused image. We tested our method using different resolution satellite images of dense urban areas (the IKONOS, KOMPSAT-2, and TerrSAR-X , etc). To examine performance, our algorithm is evaluated both by visual and quantitative methods and compared with various other fusion algorithms. The assessments indicate that the proposed method is more flexible than the other methods, because it can provide information on selective fusion that takes regional characteristics into consideration. Future work will focus on mapping and interpretation using images enhanced by the fusion of SAR and optical images compared to those of separate SAR or optical images. We can improve the spectral information further by fusing the SAR image with multispectral (MS) image or hyperspectral (HS) image. Data acquired from slightly different orbits can be fused to produce stereo images. SAR stereo-pairs can be used to view a scene in three dimensions, very useful for geological applications, or monitoring ice movement.

REFERENCES

[1] B. Yifang, H. Hongtao, and I. M. Rangel, "Fusion of Quickbird and Radarsat SAR data for urban land cover mapping: object-based and knowledge-based approach," *Int. J. Remote Sens.*, vol. 31, no. 6, pp1391–1410, Mar. 2010.

[2] C. Pohl and J. L. Genderen, "Multisensor image fusion in remote sensing: concepts, method and applications," *Int. J. Remote Sens.*, vol 19, no. 5, pp. 823–854, Mar. 1998.

[3] F. Pacifici, F. D. Frate, W. J. Emery, P. Gamba, and J. Chanussot, "Urban mapping using coarse SAR and optical data: outcome of the 2007 GRSS data fusion," *IEEE Geosci. Remote Sens. Lett.*, vol. 5, no. 3, pp. 331–335, Jul. 2008.

[4] N. Longbotham, F. Pacifici, T. Glenn, A. Zare, M. Volpi, D. Tuia, E. Christophe, J. Michel, J. Inglada, J. Chanussot, and Q. Du, "Multi- modal change detection, application to the detection of flooded areas: outcome of the 2009–2010 data fusion contest," *IEEE J. Sel. Topics Appl. Earth Observ. Remote Sens.*, vol. 5, no. 1, pp. 331–342, Feb. 2012.

[5] M. Mahta, L. D. Jennifer, and A. Steven, "Forest variable estimation from fusion of SAR and multispectral optical data," *IEEE Trans. Geosci. Remote Sens.*, vol. 40, no. 10, pp. 2176–2187, Oct. 2002.

[6] A. Vidal and M. R. Moreno, "Change detection of isolated housing using a new hybrid approach based on object classification with op- tical and Terrasar-X data," *Int. J. Remote Sens.*, vol. 32, no. 24, pp. 9621–9635, Dec. 2011.

[7] S. Klonus and M. Ehlers, "Pansharpening with Terrasar-X and optical data," in *3rd TerraSAR-X Science Team Meeting*, DLR Oberpfaffen-hofen, Germany, Nov. 25–26, 2008 [Online]. Available: http://sss.ter-rasar-x.dlr.de/accessed 2012/04/28

[8] L. Alparone, S. Baronti, A. Garzelli, and F. Nencini, "Landsat ETM+ and SAR image fusion based on generalizatied intensity modulation," *IEEETrans. Geosci. Remote Sens.*, vol. 42, no. 12, pp. 2832–2839, Dec. 2004.

[9] Y. Chibani, "Integration of panchromatic and SAR features into multispectral spot images using 'à trous' wavelet decompostion," *Int.J. Remote Sens.*, vol. 28, no. 10, pp. 2295–2307, May 2007.

[10] G. Hong, Y. Zhang, and B. Mercer, "A wavelet and his integration method to fuse high resolution SAR with moderate resolution multi-spectral images," *Photogramm. Eng. Remote Sens.*, vol. 75, no. 10, pp. 1213–1223, Oct. 2009.

[11] J. Zhang, J. Yang, Z. Zhao, H. Li, and Y. Zhang, "Block-regression based fusion of optical and SAR imagery for feature enhancement," *Int. J. Remote Sens.*, vol. 31, no. 9, pp. 2325–2345, May 2010.

[12] S. Chen, H. Su, R. Zhang, J. Tian, and J. Xia, "Scaling between Landsat-7 and SAR images based on ensemble empirical mode de-composition," *Int. J. Remote Sens.*, vol. 33, no. 3, pp. 826–835, Feb. 2012.

[13] Y. Dong, B. Forster, and C. Ticehurst, "Radar backscatter analysis for urban environments," *Int. J. Remote Sens.*, vol. 18, no. 6, pp. 1351–1364, Mar. 1997.

[14] T. Hong and R. Schowengerdt, "A robust technique for precise registra-tion of radar and optical satellite images," *Photogramm. Eng. Remote Sens.*, vol. 71, no. 5, pp. 585–593, May 2005.

[15] J. Lee, "Digital image enhancement and noise filtering by use of local statistics," *IEEE Geosci. Pattern Anal. Machine Intell.*, vol. 2, no. 2, pp. 165–168, Mar. 1980.

[16] H. Chen, M. Arora, and P. Varshney, "Mutual information-based reg-istration for remote sensing data," *Int. J. Remote Sens.*, vol. 24, no. 18, pp. 3701–3706, Sep. 2003.

[17] S. Kirkpatrick, C. D. Gelatt, and M. P. Vecchi, "Optimization by sim-ulated annealing," *Science*, vol. 22, no. 4598, pp. 671–680, May 1983.

[18] Y. Han, Y. Byun, J. Choi, D. Han, and Y. Kim, "Automatic registra-tion of high-resolution images using local properties of features," *Pho-togramm. Eng. Remote Sens.*, vol. 78, no. 3, pp. 211–221, Mar. 2012.

ISSN (ONLINE) : 2395-695X
ISSN (PRINT) : 2395-695X
Available online at www.ijarbest.com
International Journal of Advanced Research in Biology, Ecology, Science and Technology (IJARBEST)
Vol. 1, Issue 8, November 2015

[19] P. Reinartz, R. Müller, P. Schwind, S. Suri, and R. Bamler, "Orthorectification of VHR optical satellite data exploiting the geometric accuracy of TerraSAR-X data," *ISPRS J. Photogramm. Remote Sens*, vol. 66, no. 1, pp. 124–132, Jan. 2011.

[20] R. Perko, H. Raggam, K. Gutjahr, and M. Schardt, "Using worldwide available Terrasar-X data to calibrate the geo-location accuracy of op- tical sensors," in *Proc. 2011 IEEE IGARSS*, Vancouver, Canada, pp. 2551–2554.

[21] S. Suri and P. Reinartz, "Mutual-information-based registration of Terrasar-X and IKONOS imagery in urban areas," *IEEE Trans. Geosci. Remote Sens.*, vol. 48, no. 2, pp. 939–949, Feb. 2010.

[22] R. M. Haralick, K. Shanmugam, and I. Dinstein, "Textural features of image classification," *IEEE Trans. Syst., Man, Cyber.*, vol. 3, no. 6, pp. 610–621, Nov. 1973.

[23] X. Wu, "Adaptive split-and-merge segmentation based on piecewise least-square approximation," *IEEE Trans. Pattern Anal. Machine Intell.*, vol. 25, no. 8, pp. 808–815, Nov. 1993.

[24] S. Mallet and A. Wavelet, *Tour of Signal Processing*. New York, NY, USA: Academic, 1998.

[25] S. Mallat, "A theory for multiresolution signal decomposition: The wavelet representation," *IEEE Pattern Anal. Machine Intell.*, vol. 11, pp. 674–693, Jul. 1989.

[26] S. Li, J. T. Kwok, and Y. Wang, "Using the discrete wavelet frame transform to merge Landsat TM and spot panchromatic images," *Inf. Fusion*, vol. 3, no. 1, pp. 17–23, Mar. 2002.

[27] J. Núnez, X. Otazu, O. Fors, A. Pardes, V. Pala, and R. Arbiol, "Multiresolution-based image fusion with additive wavelet decompositon," *IEEE Trans. Geosci. Remote Sens.*, vol. 37, no. 3, pp. 1204–1211, May 1999.

[28] R. C. Gonazalez and R. E. Woods, *Digital Image Processing*. Englewood Cliffs, NJ, USA: Prentice-Hall, 2002.

[29] T. M. Tu, C. L. Hsu, P. Y. Tu, and C. H. Lee, "An adjustable PAN-sharpening approach for IKONOS/QuickBird/GeoEye-1/Worldview-2 imagery," *IEEE J. Sel. Topics Appl. Earth Observ. Remote Sens.*, vol. 5, no. 1, pp. 125–134, Feb. 2012.

[30] L. Alparone, L. Wald, J. Chanussot, C. Thomas, P. Gamba, and L. M. Bruce, "Outcome of the 2006 GRS-S data-fusion contest," *IEEE Trans. Geosci. Remote Sens.*, vol. 45, no. 10, pp. 3012–3021, Oct. 2007.

[31] F. Palsson, J. R. Sveinsson, J. A. Benediktsson, and H. Aanaes, "Classification of pansharpened urban satellite images," *IEEE J. Sel. Topics Appl. Earth Observ. Remote Sens.*, vol. 5, no. 1, pp. 281–297, Feb. 2012.

[32] J. Choi, J. Yeom, A. Chang, Y. Byun, and Y. Kim, "Hybrid pansharpening algorithm for high-spatial resolution satellite imagery to improve spatial quality," *IEEE Geosci. Remote Sens. Lett.*, vol. 10, no. 3, pp. 490–494, May 2013.

[33] J. Choi, D. Han, and Y. Kim, "Context-adaptive pansharpening algorithm for high-resolution satellite imagery," *Can. J. Remote Sens.*, vol. 38, no. 1, pp. 109–124, Feb. 2012.

[34] M. M. Khan, L. Alparone, and J. Chanussot, "Pansharpening quality assessment using the modulation transfer functions of instruments," *IEEE Trans. Geosci. Remote Sens.*, vol. 47, no. 11, pp. 3880–3891, Nov. 2009.

[35] S. Rahmani, M. Strait, D. Merkurjev, M. Moeller, and T. Wittman, "An adaptive IHS PAN-sharpening method," *IEEE Geosci. Remote Sens. Lett.*, vol. 7, no. 4, pp. 746–750, Oct. 2010.

[36] L. Alparone, S. Baronti, A. Garzelli, and F. nencini, "A global quality measurement of PAN-sharpened multispectral imagery," *IEEE Geosci. Remote Sens. Lett.*, vol. 1, no. 4, pp. 313–317, Oct. 2004.

[37] S. Yang, M. Wang, and L. Jiao, "Fusion of multispectral and panchromatic images based on support value transform and adaptive principal component analysis," *Inf. Fusion*, vol. 13, no. 3, pp. 177–184, Jul. 2012.

[38] J. Zhou, D. Civco, and J. Silander, "A wavelet transform method to merge Landsat TM and spot panchromatic data," *Int. J. Remote Sens.*, vol. 19, no. 4, pp. 743–758, Feb. 1998.